Songklanakarin J. Sci. Technol.
41 (3), 529-538, May – Jun. 2019

http://www.sjst.psu.ac.th

Original Article

Simulation of temperature distribution in different human skin types exposed to laser irradiation with different wavelengths and laser irradiation intensities

Patcharaporn Wongchadakul[1], Phadungsak Rattanadecho[1*], and Teerapot Wessapan[2]

[1] *Center of Excellence in Electromagnetic Energy Utilization in Engineering, Faculty of Engineering, Thammasat University, Rangsit Campus, Khlong Luang, Pathum Thani, 12120 Thailand*

[2] *School of Aviation, Eastern Asia University, Khlong Luang, Pathum Thani, 12110 Thailand*

Received: 17 January 2017; Revised: 6 December 2017; Accepted: 26 December 2017

Abstract

In modern medical facilities, laser technology is becoming more important in aesthetic and medical applications. However, inappropriate laser irradiation can result in harmful effects such as thermal burn injury. This occurs because thermal response of the skin due to laser irradiation is not well understood. In this study, the thermal response of skin to laser radiation was investigated under the effects of wavelength, laser intensity, and incident time. The transient bioheat model was considered and solved numerically using the finite element method. This study demonstrated that the skin temperature distribution depends strongly on the wavelength, intensity, and skin color type. The amount of energy absorption is significantly higher in the shorter wavelength range and with increasing intensity. Further, a darker skin color results in higher laser absorption. The obtained values provide an indication of the limitations that must be considered during laser-induced thermotherapy.

Keywords: laser, bioheat equation, skin, finite element, thermotherapy

1. Introduction

Lasers have become extremely important treatment devices in the field of engineering and dermatology (Carroll & Humphreys, 2006; Gould, 1959; Maiman, 1960; Zaret *et al.*, 1961). Recently, they have been used for a variety of applications, ranging from surgical operations and the treatment of skin disease to cosmetic dermatology. In comparison to traditional methods, laser irradiation is more effective and reliable featuring small wound and quick recovery (Carroll & Humphreys, 2006). In these treatments, the most important issue is to control the increase in temperature and distribution of the temperature in the living tissue. This will lower the unwanted thermal damage to surrounding tissue. The thermal response of tissue to laser light depends on the thermal and optical properties, light source, and duration of exposure. In laser thermotherapy, prediction of a safe dosage of laser light and irradiation time for tissue can be predicted accurately using numerical simulation techniques before application of the treatment (Carroll & Humphreys, 2006). Indeed, the Pennes bioheat equation is widely used for numerical simulation of laser thermotherapy. This equation was introduced by Pennes (1998), which is basically a heat diffusion equation incorporating the effect of blood perfusion in capillaries and metabolic heat generation due to metabolism.

Recently, thermal models of biological tissue have been rapidly developed and have been used extensively in studies of dermatological implications during exposure to laser irradiation and prediction of therapeutic responses to laser irradiation. Dua and Chakraborty (2005) numerically investigated the damage to biological tissues when they were subjected to single-point laser or diathermy. Jaunich, Raje,

*Corresponding author
Email address: ratphadu@engr.tu.ac.th

Kim, Mitraand, and Guo (2008) analyzed the temperature distributions and heat-affected zone in skin tissue when it was irradiated by a focused laser beam from a short pulse laser source. Lee and Lu (2004) carried out a numerical analysis of heat transfer in a 3D skin tissue model with an embedded vascular system. In their study, tissue and blood temperatures in arterial and venous vessels were solved by using the bioheat equation. Chen, Liang, Zhu, Sun, and Wang (2014) carried out a numerical calculation solution of the finite element method (FEM) of a skin tissue after laser irradiation at four wavelengths: 532, 694, 755, and 800 nm. In particular, the change in temperature in perfused tissue due to diffusion of blood in the tissue and metabolic heat generation of any biological sample could be accurately predicted by Pennes' bioheat equation. However, this equation fails to predict correct temperature distribution in vascularized tissue featuring large blood vessels. In such a situation, the effect of blood flow in relatively large diameter vessels and on tissue temperature can be determined using combined momentum and energy conservation equations in the vascular domain and Pennes' bioheat equation in the tissue domain. However, the present study considered a region of skin far from large diameter blood vessels. The above assumption concurs with Bhowmik *et al.* (2015) featuring the effect of focused laser light on perfused tissue and that of focused ultrasound on vascularized tissue. In fact, the rise in temperature and quantification of the thermal damage in the skin and tumor due to focused laser light was determined by a combination of the bioheat equation, laserlight attenuation, and thermal damage equation.

However, most studies have mainly focused on the modeling and influence of specific parameters such as the wavelength. In fact, there is a scarcity of systematic studies that consider the effects of operating parameters such as laser wavelength, laser irradiation intensity, type of tissue, and irradiation time on the heat transfer in layered skin. These parameters directly affect the therapeutic effectiveness during the treatment. In practical situations, these effects enhance the heat transfer and absorption process within the target tissue which can cause changes in temperature within the tissue. Therefore, in order to provide adequate information on the appropriate level of laser transition from a laser instrument, it is essential to consider all of the previously mentioned parameters in the analysis.

The objective of this research was to model the laser-tissue interaction related to medical applications by understanding the thermal response of tissue to laser irradiation. The aim is to minimize unwanted side effects from the thermal damage and provide a basis for new treatment strategies by proposing prediction and evaluation methods by developing models and simulation tools. The effects of the laser wavelength, laser intensity, type of tissue, and irradiation time on heat transfer during laser-induced thermotherapy in the layers of skin were systematically investigated.

2. Formulation of the Problem

According to the biological structure of skin, it is divided into three layers: epidermis, dermis, and subcutaneous tissue (Odland & Goldsmith, 1991). When the skin tissue is exposed to laser irradiation, the temperature gradient within the layers of the outer skin, epidermis, and dermis play an important role in the heat conduction. This study determines the effects of the operating parameters on the heat transfer in the layers of skin during laser irradiation.

3. Methods and Model

The study focuses on the heat transfer characteristics of skin subjected to a laser beam in different therapeutic situations. The numerical simulation is analyzed by FEM on COMSOL Multiphysics software. The temperature changes in the layers of skin due to the energy absorbed were described by the Beer-Lambert's law and Pennes' bioheat equation.

3.1 Physical model

A two-dimensional (2D) axisymmetrical model of the layers of skin was developed based on a physical model in previous research (Li, Li, Huang, & Xu, 2010). Figure 1 shows the three-dimensional (3D) and 2D planes of the skin model used in this study. The skin model can be simplified to 2D plane or axisymmetric analytical problem instead of a 3D simulation model for quick modeling and an efficient analysis to meet the timing in computational simulation. Although the skin is a complex heterogeneous tissue, it is common to approximate skin as a 2D skin model constructed in an axial symmetrical plane with three different layers (epidermis, dermis, and subcutaneous tissue) as illustrated in Figure 1(b). It supposes that the laser spot shape is circular and the direction of the laser irradiation is perpendicular to the skin. It was also assumed that the tissue was approximately uniform within each layer, which meant that the thermal and optical properties were not different within a particular layer of tissue. Table 1 gives the thicknesses and thermal and optical properties used in this study (Aguilar, Diaz, Lavernia, & Nelson, 2002; Bhowmik, Pepaka, Mishra, & Mitra, 2015; Chen, Liang, Zhu, Sun, & Wang, 2014; Tseng, Bargo, Durkin, & Kollias, 2009).

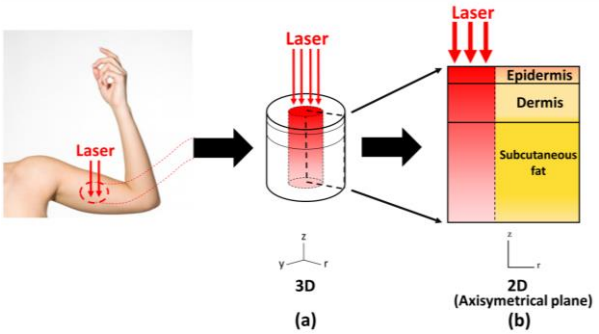

Figure 1. The skin model: (a) 3D skin model with laser irradiation, (b) 2D skin model with laser irradiation.

3.2 Mathematical modeling

Temperature distributions within the layers of skin were obtained by solving Pennes' bioheat equation (Pennes, 1998). The transient bioheat equation effectively describes how heat transfer occurs within the skin, and the equation can be written as:

$$\rho C\frac{\partial T}{\partial t}=\frac{d}{dz}\cdot\left(k\frac{dT}{dz}\right)+\frac{d}{dr}\cdot\left(k\frac{dT}{dr}\right)+\rho_b C_b\omega_b(T_b-T)+Q_{met}+Q_{Laser} \quad (1)$$

where ρ is the tissue density (kg/m^3), C is the heat capacity of tissue (J/kg K), k is the thermal conductivity of tissue (W/m K), T is the tissue temperature (°C), T_b is the temperature of blood (°C), ρ_b is the density of blood (kg/m^3), C_b is the specific heat capacity of blood (J/ kg K), ω_b is the blood perfusion rate (1/s),Q_{met} is the metabolic heat generation (W/m^3), and Q_{Laser} is the external heat source term related to laser irradiation (W/m^3).

In the analysis, heat convection between the tissue and blood flow is approximated by the blood perfusion term $\rho_b C_b \omega_b (T_b - T)$.

To simplify the problem, the following assumptions were made:

1. Each layer of skin tissue is a bio-material with constant thermal properties and optical parameters within the same layer.
2. There is no phase change of substance in the tissue.
3. There is no chemical reaction in the tissue.
4. A 2D skin model constructed in an axial symmetrical plane is assumed.
5. Unsteady heat transfer is considered.
6. The contact surface between tissues is in a smooth condition.
7. The effect of shrinkage is negligible.
8. All tissues are homogeneous and isotropic.
9. The laser deposition term in the tissue follows Beer-Lambert's law.

The boundary conditions and the physical domain are indicated in Figure 2. The upper surface of the skin (z = 0) is considered to be under a convective boundary condition:

Table 1. Thermal properties and optical properties of tissues (Bhowmik *et al*., 2015; Chen *et al*., 2014; Aguilar *et al*., 2002; Tseng *et al*., 2009)

		Dermis	Subcutaneous fat
Thickness (mm)	0.05	1.95	10
Tissue density, ρ (kg/m^3)	1200	1090	1210
Specific heat of tissue, C (J/kg.K)	3950	3350	2240
Thermal conductivity, k (W/(m.K))	0.24	0.42	0.194
Blood perfusion, ω_b (1/s)	0	0.0031	0.0031
Metabolic heat generation, Q_{met} (W/m^3)	368	368	368
Absorption coefficient, a(1/m), 532 nm (I-II)	Tseng *et al*.,2009	Aguilar *et al*.,2002	Aguilar *et al*.,2002
Absorption coefficient, a(1/m), 755 nm (I-II)	Tseng *et al*.,2009	Aguilar *et al*.,2002	Aguilar *et al*.,2002
Absorption coefficient, a(1/m), 800 nm (I-II)	Tseng *et al*.,2009	Aguilar *et al*.,2002	Aguilar *et al*.,2002
Absorption coefficient, a(1/m), 755 nm (V-VI)	Tseng *et al*.,2009	Aguilar *et al*.,2002	Aguilar *et al*.,2002
Absorption coefficient, a (1/m), 800 nm (V-VI)	Tseng *et al*.,2009	Aguilar *et al*.,2002	Aguilar *et al*.,2002
The width of the irradiated area, σ (mm)		5	
Ambient temperature, T_{am}(°C)		25	
Initial temperature, T_0 (°C)		36	
Blood temperature ,T_b (°C)		36	
Heat convection coefficient, h(W/m^2.K)		10	
Blood density, ρ_b (kg/m^3)		1060	
Specific heat of blood, C_b (J/kg.K)		3660	
Intensity, I (W/mm^2)		1, 1.5, 2	

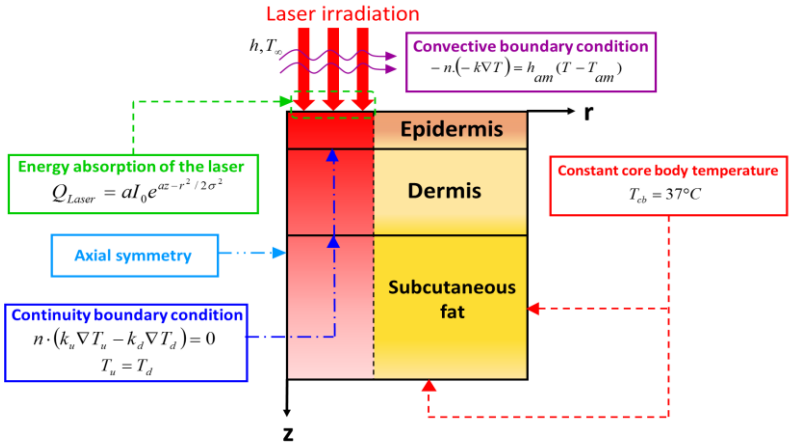

Figure 2. Boundary conditions and physical domain.

$$-kdT/dz = h_{am}(T - T_{am}) \quad (2)$$

where T_{am} is the ambient temperature (°C) and h_{am} is the convective coefficient of the air (W/m^2 K).

The outer surface of the skin tissue, except for the upper surface, is considered to be under a constant core body temperature (T_c),

$$T_c = 37\ °C,\ t \geq 0\ s \quad (3)$$

It is assumed that no contact resistance occurs between the internal layers of the three layers of skin (epidermis, dermis, and subcutaneous tissue). Therefore, the internal boundaries are assumed to be under a continuity boundary condition,

$$n \cdot \left(k_i \nabla T_i - k_j \nabla T_j\right) = 0 \quad (4)$$

where i is any layer and j is the adjacent layer to i. Therefore, i = 1, 2 and j =2, 3.

Considering the laser beam irradiation, the boundary condition will be applied on the boundary of the model in the direction of the laser beam in order to simplify the solution. Therefore, the laser intensity along tissue depth (z) is described by Beer-Lambert's law as follows:

$$I(z) = I_0 e^{-az} \quad (5)$$

The energy absorption of the laser irradiation can be expressed as follows:

$$Q_{Laser} = aI_0 e^{az - r^2/2\sigma^2} \quad (6)$$

where I is the laser irradiation intensity (W/m^2), $I_0$is the irradiation intensity at the skin surface (W/m^2), a is the absorptivity of the tissue (1/m), z is the depth of tissue, and σ is the width of the irradiated area (mm).

In this study, the absorption coefficient of the laser in the epidermis of the skin is taken from Tseng, Bargo, Durkin, and Kollias (2009), while the absorption coefficients of the dermis and subcutaneous fat are taken from Chen, Liang, Zhu, Sun, and Wang (2014) (Table1).

3.3 Numerical procedure

Heat generation is determined by the optical properties of the tissue and laser parameters. They are primarily the irradiance, irradiation time, and absorption coefficient. The coefficient itself is a function of the laser wavelength. Heat transport is solely characterized by the thermal properties of the tissue such as heat conductivity and heat capacity. In addition, the effects of heat depend on the type of tissue and the temperature reached inside the tissue (Alster & Lupton, 2001; Fodor, Elman, & Ullmann, 2011). In this study, the bioheat equation and related boundary conditions were numerically simulated using finite element solver, COMSOL Multiphysics software.

The 2D geometry is discretized using triangular elements. A convergence test of the wavelength (532 nm), intensity (1.5 W/mm^2), and the various properties listed in Table 1 was carried out to identify the number of elements required. The convergence test leads to a grid with approximately 40,000 elements. It is reasonable to confirm that, for this number of elements, the accuracy of the simulation results is independent from the number of elements.

4. Results and Discussion

In this study, the effects of laser light wavelength, incident time, laser intensity, and type of skin color on the temperature distributions in the layered skin during laser thermotherapy are systematically examined. Here, the mathematical model was composed of the bioheat equation and Beer-Lambert's law. These equations were solved simultaneously for different therapeutic situations (Cvetkovic, Poljak, & Peratta, 2010; Gheitaghy, Takabi, & Alizadeh, 2014; Tung, Trujillo, López, Rivera, & Berjano, 2009). The following discussion focuses on the heat transfer in the three layers of skin tissue during laser-induced thermotherapy (non-ablative laser irradiation). In this study, wavelengths of 532, 755, and 800 nm were selected. These wavelengths were taken from actual clinical procedures (Patil & Dhami, 2008; Trivedi, Wall, 2007; Yang, & Cho, 2017). It was assumed that the output of the laser is continuous. Further, laser irradiation intensities of 1, 1.5, and 2 W/mm^2 were selected. It was supposed that the laser beam is circular and that the laser irradiates the skin perpendicularly. In this study, the thicknesses of the epidermis, dermis, and subcutaneous fat are set as 0.05, 1.95, and 10 mm, respectively, and the radius of the domain is 10 mm.

Melanin functions as an absorptive pigment, which is ordinarily contained within the epidermis layer of the skin. It is an effective absorber of light and is able to select light color (wavelength) absorption (Nouri, 2011; Patil & Dhami, 2008). The absorption results in a reduction in energy and is transformed into thermal energy and finally results in increased temperature. The size, shape, and density of melanin particles are factors in determining the degree of opacity or skin color (Sturm, Box, & Ramsay, 1998). Darker skin contains more melanin (Yamaguchi, Brenner, & Hearing, 2007). Therefore, a darker skin can absorb more energy and generate a higher temperature compared to a lighter skin. Consequently, skin color is one of the parameters in this study. Referring to Fitzpatrick's scale (Fitzpatrick, 1988), the color of the skin is separated into six types: I, II, III, IV, V, and VI, denoting white, white-beige, light brown, moderate brown, dark brown, and black colors, respectively. The skin color types I–II and V–VI are chosen in this study as they can be clearly differentiated.

For the simulation, the optical properties and thermal properties were taken directly from Table 1. In all simulations, two skin types are selected, namely skin types I–II and V–VI. We used their absorption coefficients of different wavelengths in the epidermis of the upper inner arm from Tseng, Bargo, Durkin, and Kollias (2009). Nevertheless, for all laser wavelengths, the absorption coefficients of the dermis and subcutaneous tissues were taken from Aguilar, Diaz, Lavernia, and Nelson (2002) as 0.24 (/mm) and 0.24 (/mm), respectively. The thermal properties and skin thicknesses were taken from Chen, Liang, Zhu, Sun, and Wang (2014) and metabolic heat generation was taken from Bhowmik, Repaka, Mishra, and Mitra (2015) (Table1).

4.1 Verification of the model

In order to verify the accuracy of the present numerical model, a modified case of the simulated results was then validated against the numerical results with the same geometric model obtained by He, Minoru, Ryu, Himeno, and Kawamura (2004). The axially symmetrical case of two-layer skin tissue with a cancerous tumor is used in the validation case. In the validation case, the skin is exposed to laser irradiation with an intensity of 1.4 W/mm^2. The results of the selected test case are illustrated in Figure 3 for the temperature distribution in the skin with a cancerous tumor. Good agreement of the temperature distribution with elapsed times between the present solution and that of He, Minoru, Ryu, Himeno, and Kawamura (2004) was clearly shown. This favorable comparison gives confidence in the accuracy of the present numerical model. It is important to note that some errors possibly occurred in the simulations generated by the input thermal properties, optical properties, and numerical scheme.

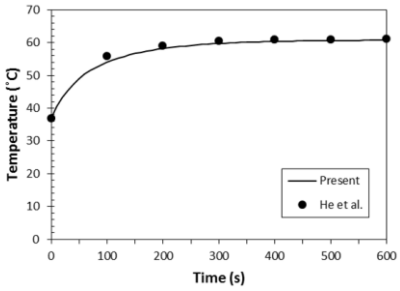

Figure 3. Comparison of the calculated temperature distribution with the temperature distribution obtained by He *et. al*. (2004).

4.2 Temperature distribution

Figures 4 and 5 demonstrate the temperature changes of the irradiation center with elapsed time. It can be seen from all graphs that the temperature rapidly increased in the early stage and gradually rose up afterwards and finally approached a steady-state value. The heating speed differs with different wavelengths as well as laser intensities. The laser with a wavelength of 532 nm and laser intensity of 2 W/mm^2 corresponded to the highest speed of heating up.

Figure 4 shows the skin temperature changes (at the position of z=0, r=0) with elapsed time at the different wavelengths when the skin was irradiated by a laser with intensities of (a) 1, (b) 1.5, and (c) 2 W/mm^2. The laser with a wavelength of 532 nm produced the highest temperature value for all intensity levels while the maximum temperatures at the wavelengths of 755 nm and 800 nm were not different. This is because at the wavelength of 532 nm, the skin has a greater absorption coefficient than the wavelengths of 755 nm and 800 nm. When the skin is exposed to the laser, the absorbed energy is converted into thermal energy which leads to an increased temperature. Moreover, it can be seen that greater intensity provides a faster temperature increase as well as faster heating up. Figure 8 shows the results of skin temperature changes (at the position of z=0, r=0) with elapsed time at different laser intensities when the skin is irradiated by a laser at wavelengths of 532, 755, and 800 nm. The laser with a wavelength of 532 nm had the highest maximum temperature for all intensity levels. Higher intensities provided faster temperature increases as well as faster heating up which were similar to the results illustrated in Figure 4.

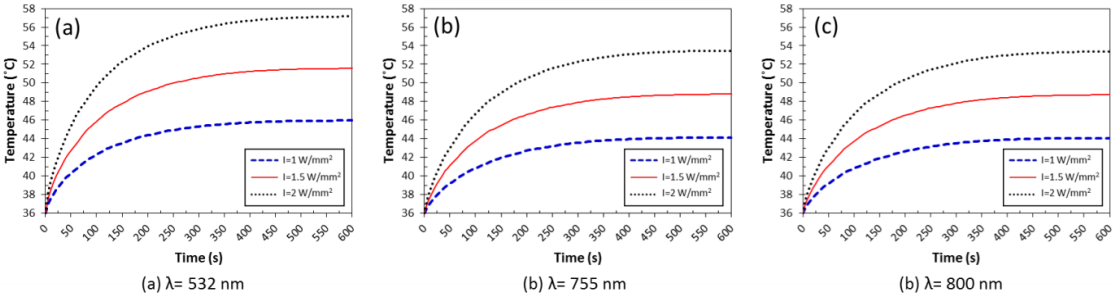

Figure 4. Temperature changes (at the position of z=0, r=0) with elapsed time at different wavelengths (532, 755, and 800 nm) for skin color type I–II under laser irradiation with intensities of (a) 1, (b) 1.5, and (c) 2 W/mm^2, respectively

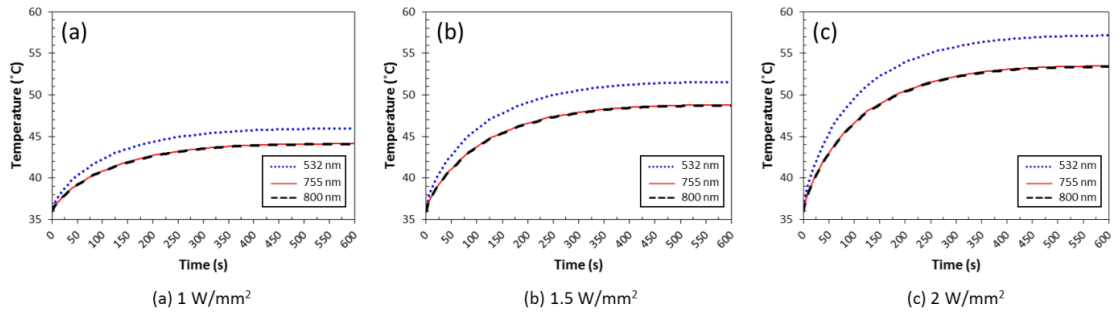

Figure 5. Temperature changes (at the position of z=0, r=0) with elapsed time at different laser intensities (1, 1.5, and 2 W/mm^2) on skin color type I–II under laser irradiation at wavelengths of (a) 532, (b) 755, and (c) 800 nm, respectively.

Figures 6 to 8 indicate the temperature fields in skin tissues after the laser-induced thermotherapy process with three different wavelengths (532, 755, and 800 nm) and with three different intensities (1, 1.5, and 2 W/mm^2) for three different durations of irradiation: 30, 60, and 600 s. Overall, these simulated results show that the increase in temperature was highest at the center of the irradiation region and decreased from the irradiation region towards the surrounding healthy tissues for all wavelengths and laser intensities after the application of laser irradiation. The effect arises from the fact that heat from the hot spot zone in the central region will diffuse to the cold region in the surrounding tissues, and in particular, the longitudinal temperature distribution affects the heat diffusion through the different layers of tissues. It is remarkable that the temperature decreases with increases in the wavelength and that the temperature in the center of the irradiation region decreases with increasing wavelength. There are two steps during laser-induced thermotherapy. First, the tissue is heated directly within the optical absorption depth. Second, heat diffusion to the deeper tissue occurs. Generally, in the early stage of laser-induced thermotherapy, the heat diffusion does not reach very deep into the tissues. After that, heat diffusion has sufficient time to spread deeper into the tissues. The temperature fields in skin tissues under each test condition occurred differently due to the effects of optical and thermal properties and absorption coefficient of the epidermal layer, which varied with wavelength. In addition, the blood perfusion rate and cooling of the skin surface also affected the temperature fields in skin as well. These parameters play an important role in releasing the excess heat in the skin.

Figure 6 represents the temperature field in the early stage of the laser-induced thermotherapy process (30 s). The skin depth heating effect causes a major part of the laser irradiation to be absorbed within the leading edge of the layered tissue for all wavelengths and laser intensities. Owning to the laser energy absorbed, the temperature distribution within the tissue decays slowly along the propagation direction, following Beer-Lambert's law as described by Equation (6). It was noted that in the case of the short wavelength (532 nm), the highest temperature values and wider hot spot areas at the skin surface occurred at all intensity levels. This is because the epidermal layer has a higher absorption coefficient value than the dermal and subcutaneous fat layers. Therefore, the outer surface, where the epidermal layer is located, can absorb more energy at this wavelength than other wavelengths because of the high absorption coefficient value.

Figure 7 presents the temperature distribution in the skin after 60 s of laser irradiation. The wavelength of 532 nm produced the highest temperature at the skin surface due to its highest absorption coefficient value. In contrast, the wavelengths of 755 and 800 nm provided greater penetration depth due to the higher thermal conductivity in the dermal layer, as evidenced by the intensity of 1W/mm^2 seen in Figure 7(a). Meanwhile the increase of the laser intensity level led to more energy absorption and caused an increase in the temperature at the skin surface because the skin surface was directly irradiated by the laser. In this case, there is not enough time for heat diffusion to take place. So the positions of the maximum temperature changes to the skin surface are shown in Figures 7 (a) and (b).

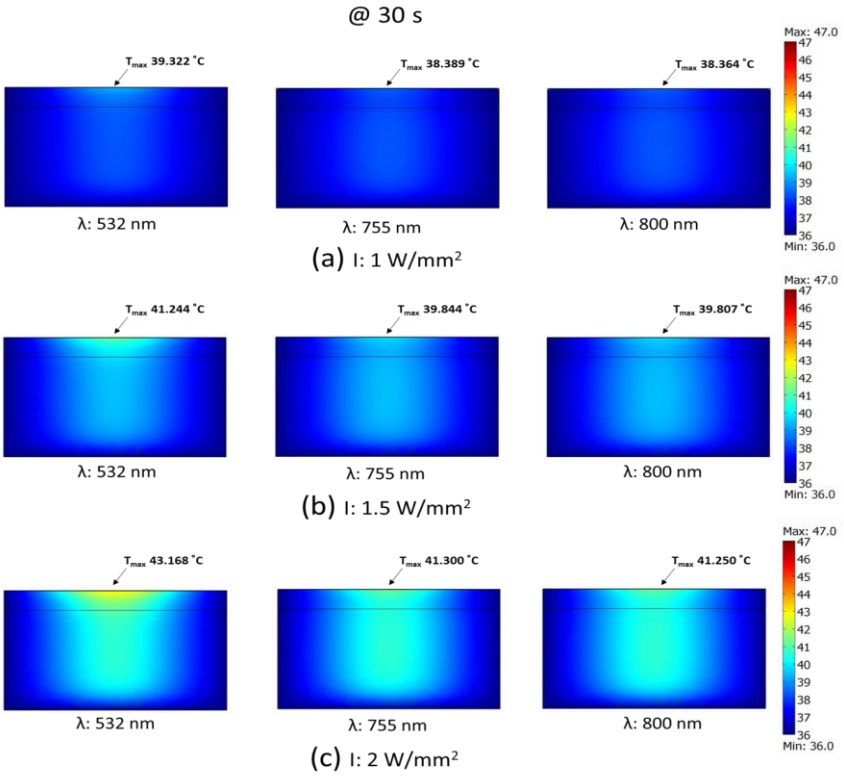

Figure 6. Temperature distribution in the skin after laser irradiation with three different wavelengths of 532, 755, and 800 nm. Laser intensities were set to (a) 1, (b) 1.5, and (c) 2 W/mm^2 (t=30 s).

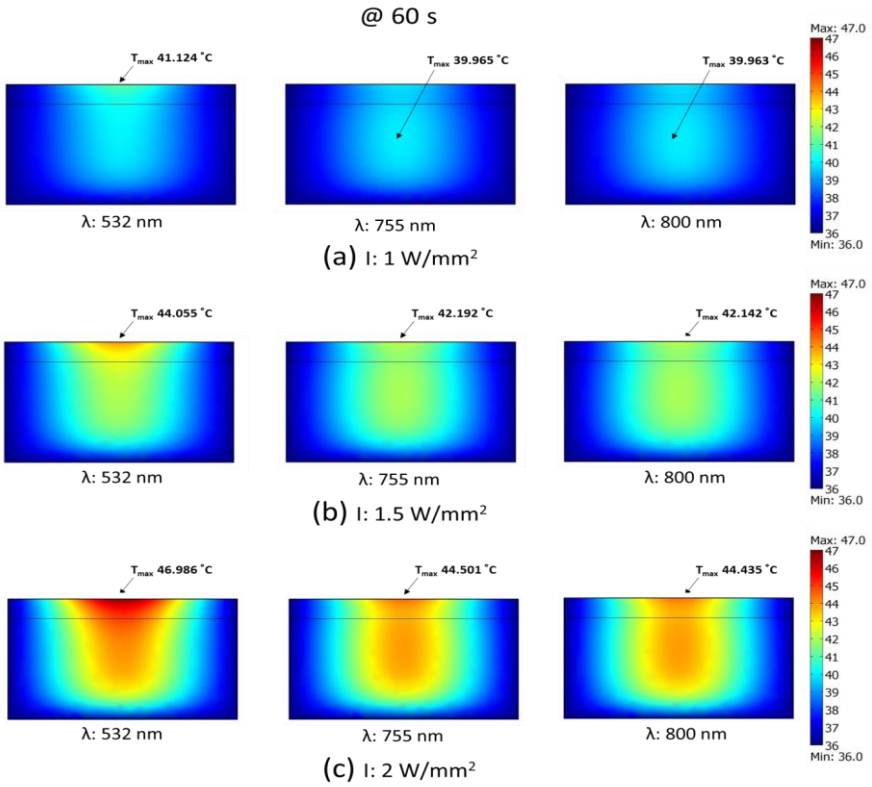

Figure 7. Temperature distribution in the skin after laser irradiation with three different wavelengths of 532, 755, and 800 nm. Laser intensities were set to (a) 1, (b) 1.5, and (c) 2 W/mm^2 (at t=60 s).

However, as time progressed (Figure 8), the wavelength of 532 nm still had the highest temperature value for all three intensities compared with wavelengths of 755 and 800 nm. Moreover, the hot spot area of the wavelength at 532 nm was wider and had a higher temperature at the skin surface as a result of its greater absorption coefficient value of the outer skin layer. After further irradiation time up to 600 s and increases in intensities up to 1.5 and 2 W/mm^2, the maximum temperature at wavelengths of 755 and 800 nm still occurred deep inside the skin layer as illustrated in Figures 8 (b) and (c). In contrast, the short wavelength always had a higher temperature at the upper surface or skin surface than the tissue deep inside the skin. This is because the effect of thermal conductivity plays an important role in the conductance of the laser energy absorbed and the irradiation time is long enough for diffusion of heat into the deeper layer. This phenomenon was not discussed in detail in previous research. In this study, the wavelengths at 532, 755, and 800 nm and laser irradiation intensities of 1, 1.5, and 2 W/mm^{2}on skin type I–II at an irradiation time of 600s served as the sole modality to enhance the thermal response in laser-induced thermotherapy throughout the treatment process without side effects on the healthy tissue in the surrounding area.

The 2D plot of temperature distribution based on a 2D axisymmetrical model of the skin layers is shown in Figure 7. The simulated temperature changes in the layers of skin in more planes, especially the hot spot zone in the layered skin under the same conditions, can again be recast in a 3D plane also under the assumption of a 2D axisymmetrical plane (Figure 9). In the figures, it can be clearly observed that the skin surface was sensitive to the thermal response during the laser-induced thermotherapy process.

5. Conclusions

Numerical simulation of the transient temperature distribution within the layers of skin tissue during laser-induced thermotherapy under different treatment conditions was performed. It was found that the temperature distribution and laser penetration depth depended strongly on the wavelength, laser irradiation intensity, and skin color type. Under the same intensity and irradiation time, an increase in the laser wavelength led to decreases in the skin temperature. It was found that the absorption of laser energy was significantly higher in the shorter wavelength range (532 nm). The level of laser intensity affects the increase in temperature within the tissues with the higher intensity level leading to a higher temperature within the tissues.

Further, a darker skin color (skin type V–VI) absorbed more laser energy. However, laser absorption by melanin in the skin decreased as the wavelength increased. The absorption coefficient of white skin (skin type I–II) is lower than that of dark skin (skin type V–VI), and therefore the dark skin color (skin type V–VI) can absorb more energy than white skin. Consequently, epidermal damage occurs more easily in dark skin types compared to white skin types. As a result, special care should be taken when treating patients with dark skin (skin type V–VI). The intensity level should be

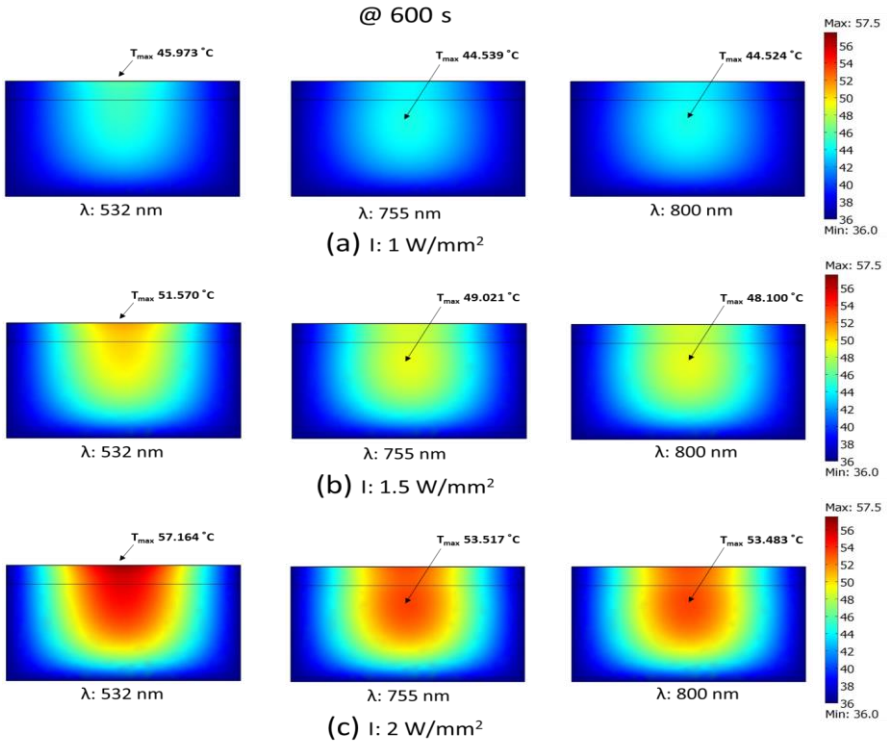

Figure 8. Temperature distribution in the skin after laser irradiation at the wavelengths of 532, 755, and 800 nm. Laser intensities were set to (a) 1, (b) 1.5, and (c) 2 W/mm^2 (t=600 s).

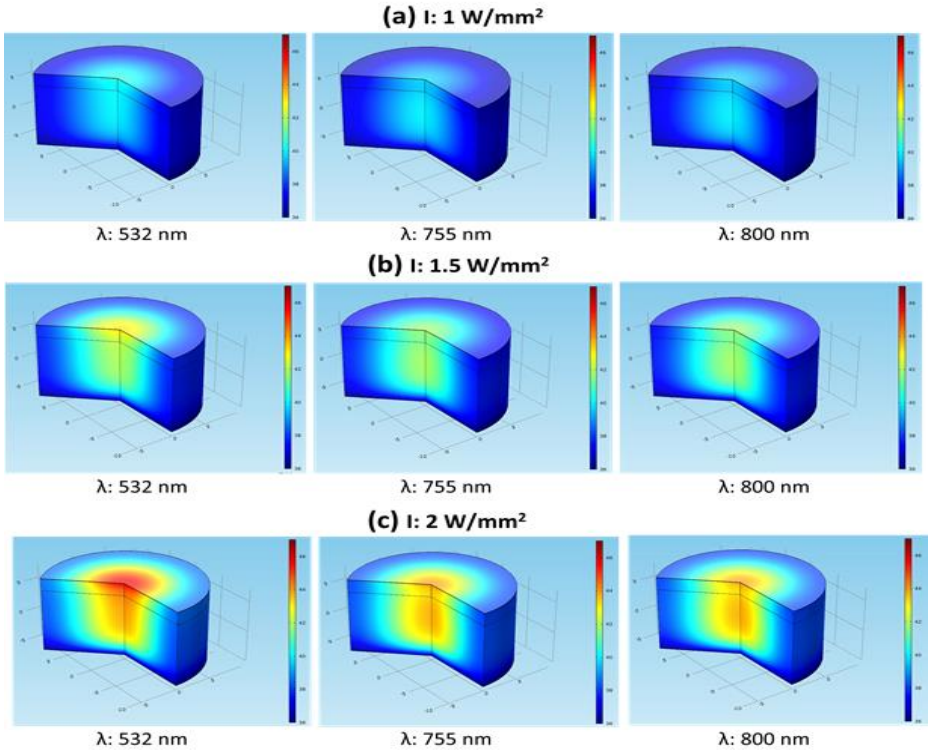

Figure 9. 3D temperature distribution in the skin after laser irradiation with three different wavelengths of 532, 755, and 800 nm Laser intensities were set to (a) 1, (b) 1.5, and (c) 2 W/mm^2 (t=60 s).

reduced in order to reduce unwanted thermal injury. Thus, as appropriate settings are necessary for highly effective and safe treatment, the proper laser for dark skin types is a longer wavelength laser because of its lower energy absorption characteristic. In addition, it was found that higher laser intensity resulted in higher absorption of laser energy by the skin. Moreover, this study also showed that the irradiation time has a marked influence on the temperature increase in the skin tissue.

The results of this study contribute to the understanding of the realistic situation and prediction of the temperature distribution in skin tissue during laser-induced thermotherapy under different treatment conditions.

From this study, it was concluded that the parameters could become significant factors to the transport phenomena in the human skin tissues when exposed to laser irradiation. However, in all cases only the bioheat theory with optical and thermal properties was performed. Thus, a more complicated theory should be developed for greater accuracy of the simulation results.

Acknowledgements

Thailand Research Fund (Contract No. RTA 5980009), Thammasat Ph.D. scholarship program and Thailand Government Budget Grant provided financial support for this research.

References

Aguilar, G., Diaz, S. H., Lavernia, E. J., & Nelson, J. S. (2002). Cryogen spray cooling efficiency. Improvement of port wine strain laser therapy through multiple-intermittent cryogen spurts and laser pulses. *Lasers in Surgery and Medicine, 31*(1), 27–35. doi:10.1002/lsm.10076

Alster, T. S., & Lupton, J. R. (2001). Lasers in dermatology. An overview of types and indications. *Clinical Dermatology, 2*(5), 291–303. doi:10.2165/00128071-200102050-00004

Bhowmik, A., Repaka, R., Mishra, S. C., & Mitra, K. (2015). Thermal assessment of ablation limit of subsurface tumor during focused ultrasound and laser heating. *Journal of Thermal Science Engineering Application, 8*(1), 011012. doi: 10.1115/1.4030731

Carroll, L., & Humphreys, T. R. (2006). Laser–tissue interactions. *Clinical Dermatology, 24*(1), 2–7. doi:10.1016/j.clindermatol.2005.10.019

Chen, K., Liang, Y., Zhu, W., Sun, X., & Wang, T. (2014). Simulation of temperature in skin under laser irradiation with different wavelengths. *Optic, 125*, 1676–1679. doi:10.1016/j.ijleo.2013.10.021

Cvetkovic, M., Poljak, D., & Peratta, A. (2010). 3D FEM temperature distribution analysis of the human eye exposed to laser radiation. *WIT Transactions on Engineering Sciences, 68*, 303-312. Retrieved from https://www.witpress.com/Secure/elibrary/papers/HT10/HT10026FU1.pdf

Dua, R., & Chakraborty, S. (2005). A novel modeling and simulation technique of photo-thermal interactions between lasers and living biological tissues undergoing multiple changes in phase. *Computers in Biology and Medicine, 35*, 447–462. doi:10.1016/j.compbiomed.2004.02.005

Fitzpatrick, T.B. (1988). The validity and practicality of sun-reactive skin types I through VI. *Archives of Dermatology, 124* (6), 869–871. doi:10.1001/archderm.1988.01670060015008

Fodor, L., Elman, M., & Ullmann, Y. (2011). *Aesthetic applications of intense pulsed light*. London, England; Springer-Verlag. doi:10.1007/978-1-84996-456-2

Gheitaghy, M., Takabi, B., & Alizadeh, M. (2014). Modeling of ultrashort pulsed laser irradiation in the cornea based on parabolic and hyperbolic heat equations using electrical analogy. *International Journal of Modern Physics C, 25*(9), 1450039. doi:10.1142/S0129183114500399

Gould, G. R. (1959). The LASER. Light amplification by stimulated emission of radiation. In P. A. Franken (Ed.), *The ann arbor conference on optical pumping. University of Michigan*, (pp. 128). Dublin, OH: OCLC

He, Y., Minoru, S., Ryu, K., Himeno, R., & Kawamura, T. (2004). Numerical and experimental study on the human blood circulation and heat transport phenomena-thermoregulation in the periphery and hyperthermia-induced tumor blood flow. *Computational Biomechanics. RIKEN Symposium*, 97–119 (in Japanese). Retrieved from http://www.compbio.riken.jp/1/download/files/HE_YING-NAIYOU.pdf

Jaunich, M., Raje, S., Kim, K., Mitraand, K., & Guo, Z. (2008). Bio-heat transfer analysis during short pulse laser irradiation of tissues. *International Heat and Mass Transfer, 51*(23–24), 5511–5521. doi:10.1016/j.ijheatmasstransfer.2008.04.033

Lee, S. L., & Lu, Y. H. (2014). Modeling of bioheat equation for skin and a preliminary study on a noninvasive diagnostic method for skin burn wounds. *Journal of the International Society for Burn Injuries, 40*(5), 930–939. doi:10.1016/j.burns.2013.10.013

Li, C., Li, S., Huang, Z., & Xu, W. (2010). Skin thermal effect by FE simulation and experiment of laser ultrasonics. *Applied Mechanics and Materials, 24-25*, 281–286. doi:10.4028/www.scientific.net/AMM.24-25.281

Maiman, T. (1960). Optical and microwave-optical experiments in ruby. *Physics, 4*, 564–6. doi:10.1103/PhysRevLett.4.564

Nouri K. (2011). Laser in dermatology and medicine. NY, New York: Springer London Dordrecht Heidelberg. Retrieved from http://www.springer.com

Odland, G. F., & Goldsmith, L. A. (1991). *Structure of the skin. Physiology, biochemistry and molecular biology of the skin* (2nd Ed.). New York, NY: Oxford University Press.

Patil, U. A., & Dhami, L. D. (2008). Overview of lasers. *Indian Journal of Plastic Surgery, 41*(3), 101–113.

Pennes, H. H. (1998). Analysis of tissue and arterial blood temperatures in the resting human forearm (reprint of 1948 article). *Applied Physiology, 85*, 5–34. Retrieved from http://jap.physiology.org/content/jap/85/1/5.full.pdf

Sturm, R. A., Box, N. F., & Ramsay, M. (1998). Human pigmentation genetics: the difference is only skin deep. *BioEssays, 20*, 712–721. doi:10.1002/(SICI)1521-1878(199809)20:9<712::AID-BIES4>3.0.CO;2-I

Trivedi, M. K., Yang, F. C. & Cho, B. K. (2017). A review of laser and light therapy in melasma. *International Journal of Women's Dermatology, 3*, 11–20. doi:10.1016/j.ijwd.2017.01.004

Tseng, S., Bargo, P., Durkin, A., & Kollias, N. (2009). Chromophore concentrations. Absorption and scattering properties of human skin in vivo. *Optics Express, 17*, 14599–14617. doi:10.1364/OE.17.014599

Tung, M. M., Trujillo, M., López, M. J. A., Rivera, M. J., & Berjano, E. J. (2009). Modeling the heating of biological tissue based on the hyperbolic heat transfer equation. *Mathematical and Computer Modelling, 50*, 665–672. doi:arXiv:0811.3359

Wall, T. L. (2007). Current concepts: Laser treatment of adult vascular lesions. *Seminar of Plastic Surgery, 21*(3), 147–158. doi:10.1055/s-2007-991183

Yamaguchi, Y., Brenner, M., & Hearing, V. J. (2007). The regulation of skin pigmentation. *The Journal of Biological Chemistry, 282*(38), 27557-27561. doi:10.1074/jbc.R700026200

Zaret, M. M., Breinin, G. M., Schmidt, H., Ripps, H., Siegel, I. M., & Solon, L. R. (1961). Ocular lesions produced by an optical maser (laser). *Science, 134*, 1525-1526. doi:10.1126/science.134.3489.1525